Accepted Manuscript

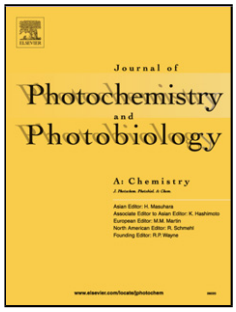

Title: Physicochemical and Photodynamic Antimicrobial Chemotherapy Activity of Morpholine-Substituted Phthalocyanines: Effect of Point of Substitution and Central Metal

Authors: Azole Sindelo, Nagao Kobayashi, Mutsumi Kimura, Tebello Nyokong

PII: S1010-6030(18)31539-9
DOI: https://doi.org/10.1016/j.jphotochem.2019.01.025
Reference: JPC 11684

To appear in: *Journal of Photochemistry and Photobiology A: Chemistry*

Received date: 25 October 2018
Revised date: 21 January 2019
Accepted date: 24 January 2019

Please cite this article as: Sindelo A, Kobayashi N, Kimura M, Nyokong T, Physicochemical and Photodynamic Antimicrobial Chemotherapy Activity of Morpholine-Substituted Phthalocyanines: Effect of Point of Substitution and Central Metal, *Journal of Photochemistry and amp; Photobiology, A: Chemistry* (2019), https://doi.org/10.1016/j.jphotochem.2019.01.025

Physicochemical and Photodynamic Antimicrobial Chemotherapy Activity of Morpholine-Substituted Phthalocyanines: Effect of Point of Substitution and Central Metal

Azole Sindelo,[a] Nagao Kobayashi,[b] Mutsumi Kimura[b] and Tebello Nyokong[a]*

[a]*Centre for Nanotechnology Innovation, Department of Chemistry, Rhodes University, Grahamstown 6140, South Africa.*

[b]Department of Chemistry and Materials, Faculty of Textile Science and Technology, Shinshu University, Ueda 386-8567, Japan

Graphical abstract

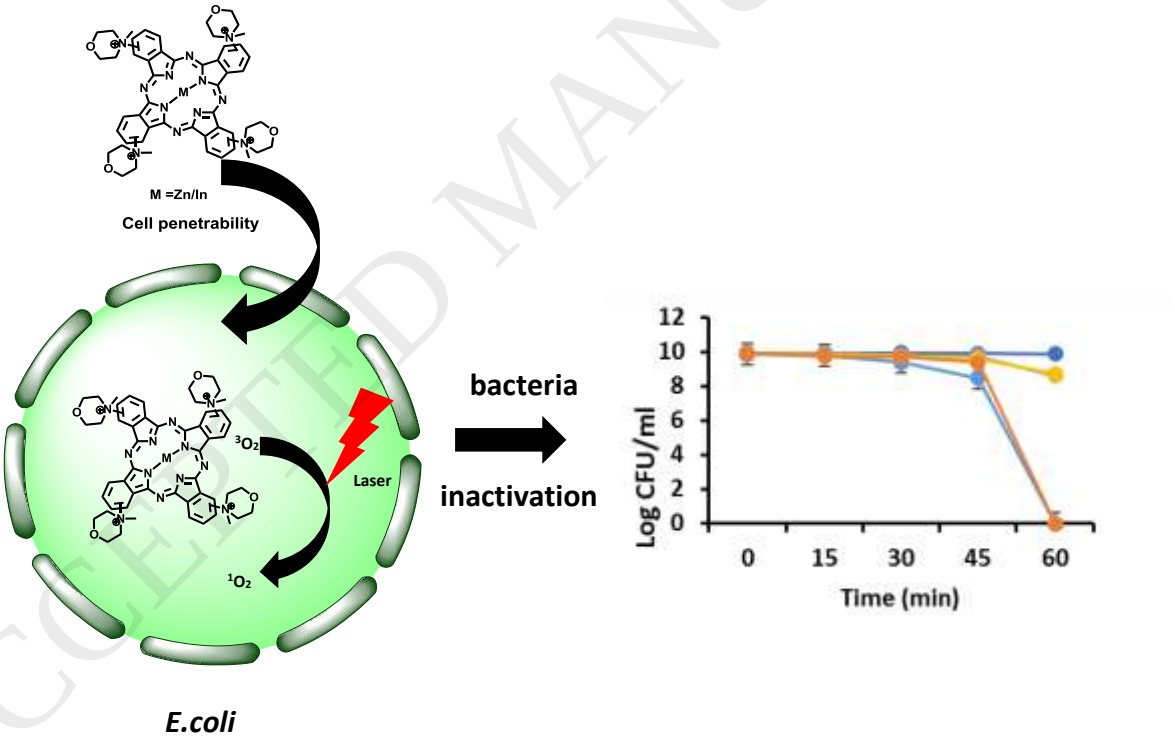

Highlights

- Zn and In tetramorpholine phthalocyanines are synthesized and then quaternized

- Photodynamic antimicrobial chemotherapy activities towards inactivation of *E. coli, S. aureus,* and *C. albican* were evaluated
- The quaternized derivatives showed total elimination of the micro-organism with log reductions greater than 9.

Abstract

In this study, novel metal-free, zinc and indium 1(4),8(11),15(18),22(25)-tetramorpholine (**1a**, **2a**, **3a** respectively) and 2(3), 9(10), 16(17),23(24)-tetramorpholine (**1b**, **2b**, **3b** respectively) phthalocyanines were synthesized and complexes **2** and **3** were quaternized. The photophysical and photochemical properties were investigated in dimethylsulfoxide. The non-peripherally substituted phthalocyanines generated higher singlet oxygen than the peripherally substituted phthalocyanines. Photodynamic antimicrobial chemotherapy activities towards inactivation of *Escherichia coli, Staphylococcus aureus* and *Candida albican* were evaluated, where all the quaternized Pcs showed total elimination of the micro-organism with log reductions greater than 9. Though the neutral Pcs had log reductions less than 2, for *C. albican* the percentage reduction was 68.5% for **2b** showing the antifungal properties of the morpholine group.

Keywords: Phthalocyanine, morpholine, photophysics, fluorescence, singlet oxygen

*Corresponding author. Tel: + 27 46 6038260; Fax: + 27 46 6225109.

1. Introduction

Phthalocyanines (Pcs) are tetra pyrrolic macrocyclic compounds with multiple attractive properties such as chemical inertness, long wavelength absorption compatible with biological window, excellent thermal and photo-stability [**1-5**]. Due to these properties, Pcs have been extensively used in various applications such as in sensors, light-emitting devices, solar cells, photodynamic therapy (photodynamic antimicrobial chemotherapy, PACT), non-linear optical materials, and catalysis [**6-13**]. PACT is based on the administration of a non-toxic photosensitizer to the microbial cells followed by activation by light of appropriate wavelength [**14-16**]. The photoexcited photosensitizer produces reactive oxygen species (ROS) such as radicals and singlet oxygen (through Type I or Type II mechanism) that are cytotoxic to the targeted bacteria [**14,15**]. MPcs are efficient photosensitizers for PACT [**16**]. The quaternized forms of In tetra pyridyloxy phthalocyanines have been employed for the photoinactivation of different types of bacteria and fungi [**17,18**]. It has been reported that cationic phthalocyanines are more effective than neutral and anionic Pcs against the Gram (-) bacteria such as *E.coli* [**19**]. Gram (-) bacteria have a thick cell wall, which is absent in Gram (+) bacteria such as *S. aureus* [**19**]. Hence in this work we employ morpholine substituted Pcs which can easily be quaternized. In addition, morpholine derivatives are well known antimicrobial agents [**20**] hence the combination of a Pc and morpholine is expected to result in improved PACT activity.

To maximise the photophysical and photochemical properties of Pcs, modification of the Pc ring can be achieved by tuning the central atom. The introduction of central metals such as indium has been reported to reduce aggregation and improved solubility [**21,22**]. Furthermore, introducing substituents at the non-peripheral (α) and peripheral (β) positions improves solubility of phthalocyanines in common organic solvents. In this study, novel morpholine alpha and beta tetra-substituted phthalocyanines (complexes **1a, 1b, 2a, 2b, 3a**,

and **3b**, Scheme 1, and the quaternized derivatives of the metalled complexes: **Q2a, Q2b, Q3a**, and **Q3b,** Scheme 2) are synthesized and their PACT activity evaluated. We compare non-peripheral to peripheral substitution on the Pc ring for PACT activity.

2. Experimental

2.1 Material

Dimethyl sulfoxide (DMSO), dimethylformamide (DMF), dichloromethane (DCM), tetrahydrofuran (THF), chloroform, methanol and ethyl acetate were purchased from Merck, while deuterated chloroform ($CDCl_3$) was purchased from Associated Chemical Enterprises. Morpholine, 4-nitrophthalonitrile, 3-nitrophthalonitrile, zinc (II) acetate ($Zn(OAc)_2$), indium (III) chloride, 1,3-diphenylisobenzofuran (DPBF), anthracene-9,10-bis-methylmalonate (ADMA) and 1,8-diazabicycloundec-7-ene (DBU) were purchased from Sigma Aldrich, while dimethyl sulphate bought from Riedel-de Haen. All solvents were dried using molecular sieves. Phosphate-buffered saline (PBS) solution pH 7.4 was prepared using appropriate amounts of Na_2HPO_4 and NaOH in ultra-pure water from a Milli-Q Water system (Millipore Corp, Bedford, MA, USA). Nutrient agar and agar bacteriological BBL Muller Hinton broth were purchased from Merck, *E. coli* (ATCC 25922) from Microbiologic. *S. aureus* (ATCC 25923) and *C. albican* (ATCC 24433) were from Davies Diagnostics.

2.2 Equipment

Electronic absorption spectra of solutions were recorded on a Shimadzu UV-2550 spectrophotometer using 3 cm quartz cell cuvette. Infrared (IR) spectra were recorded on a Bruker Alpha IR (100 FT-IR) spectrophotometer. Fluorescence emission spectra were recorded on a Varian Eclipse spectrofluorimeter. Mass spectra data were collected with a Bruker AutoFLEX III Smartbeam TOF/TOF Mass spectrometer and with Bruker microTOF II mass spectrometer. The spectra were acquired using dithranol as the MALDI matrix. ^{1}H nuclear magnetic resonance spectra recorded on a Bruker AMX 600 MHz NMR spectrometer.

Triplet state quantum yields were determined using a laser flash photolysis system consisting of an LP980 spectrometer with a PMT-LP detector and an ICCD camera (Andor DH320T-25F03). The signal from a PMT detector was recorded on a Tektronix TDS3012C digital storage oscilloscope. The excitation pulses were produced using a tunable laser system consisting of an Nd:YAG laser (355 nm, 135 mJ/4–6 ns) pumping an optical parametric oscillator (OPO, 30 mJ/3–5 ns) with a wavelength range of 420–2300 nm (NT-342B, Ekspla). The absorbance of solutions of the Pcs and the ZnPc standard were ~1.5 at Q band. The solution was introduced into a 1 cm path length UV-visible spectrophotometric cell and de-aerated using argon for 15 min.

Fluorescence decay lifetimes were measured using a time-correlated single photon counting (TCSPC) setup (FluoTime 300, Picoquant GmbH). The excitation source was a diode laser (LDH-P-670 driven by PDL 800-B, 670 nm (**Q2a**, **Q2b**, **Q3a** and **Q3b**), 720 nm (**1b**, **2a** and **2b**) and 760 nm (**1a** and **3a**) 20 MHz repetition rate, 44 ps pulse width, Pico quant GmbH). Photo-irradiations for singlet oxygen quantum yield determination and antimicrobial studies were performed using a General Electric Quartz lamp (300 W). A 680 nm glass (Schott) and water filters were used to filter off ultra-violet and far infrared radiations. An interference filter

(Intor, 700 nm with a band width of 20 nm and) was additionally placed in the light path before the sample. A light dose of 24 J/cm^2 was employed. Light intensities measured with a POWER MAX 5100 (Molelectron detector incorporated) power meter.

2.3 Syntheses

2.3.1 General procedure for the synthesis of phthalonitriles (4 and 5).

3-Nitrophthalonitrile or 4-nitrophthalonitrile (1.97 g, 10 mmol) and morpholine (3.9 g, 45 mmol) were dissolved in dry DMF (25 ml) and reacted with anhydrous Na_2CO_3 (3.12 g, 30 mmol). The reaction was stirred at 100 °C, for 18 h under inert conditions, using an oil bath to maintain the temperature. The products were precipitated in water, and the yellow precipitates formed were filtered under vacuum and recrystallized with methanol. The crude products were purified further by column chromatography using alumina and eluting with ethyl acetate. Both compounds are soluble in most organic compounds (DMF, DMSO, methanol, ethyl acetate, DCM, chloroform and THF).

3-Morpholinophthalonitrile (4). Yield: 0.56 g (22.78 %). Anal calculated for $C_{12}H_{11}N_3O$, C, 67.59 %; H, 5.20 %; N, 19.71 %; found C 67.68 %; H, 4.61 %; N, 19.74 %. IR (KBr, cm^{-1}): 2967 (C-H), 2907 (CH_2), 2869 (CH_2), 2218 (C≡N), 1597, 1512 (C=C),1255, 1179, 1099 (C-O), 1038, 957, 866, 809, 723 (C-C). ^{1}H NMR ($CDCl_3$): δ (ppm), 7.49 (d, 1H), 7.14 (d, 1H), 7.07-7.03 (m, 1H), 3.80-3.77 (d, 4H, CH_2), 3.27-3.24 (d, 4H, CH_2). MALDI-TOF-MS m/z: Calc: 213.09; Found: [M+1H] = 214.10.

4-Morpholinophthalonitrile (5). Yield: 1.18 g (48.56 %). Anal calculated for $C_{12}H_{11}N_3O$, C, 67.59 %; H, 5.20 %; N, 19.71 %; found C 67.61 %; H, 4.98 %; N, 19.75 %. IR (KBr, cm^{-1}): 3109

(C-H), 2909 (CH_2), 2864 (CH_2), 2221 (C≡N), 1592, 1507 (C=C),1257, 1179, 1110 (C-O), 1037, 951, 863, 817, 718 (C-C). ^{1}H NMR ($CDCl_3$): δ (ppm), 7.60 (d, 1H), 7.15 (d, 1H), 7.05-7.02 (m, 1H), 3.90-3.87 (d, 4H, CH_2), 3.37-3.34 (d,4H, CH_2). MALDI-TOF-MS m/z: Calc: 213.09; Found: [M+1H] = 214.11.

2.3.2 General procedure for the synthesis of metal-free phthalocyanines (1a and 1b).

Compounds **4** and **5** (0.20 g, 0.94 mmol) were each mixed with 1- pentanol and DBU (0.25 ml), followed by stirring for 20 min at 360 °C. The products were precipitated with dilute HCl. The green products were filtered and further washed with water, methanol and acetonitrile. The products were further purified by column chromatography with silica gel and eluting with chloroform. Both complexes (**1a** and **1b**) are soluble in $CHCl_3$, THF, DCM, DMF and partially in DMSO

1(4),8(11),15(18),22(25)-Tetrakis-(morpholino)phthalocyanine (1a). Yield: 13 mg (7%). Anal calculated for $C_{48}H_{46}N_{12}O_4$, C, 67.43; H, 5.42; N, 19.66; found C 66.94 %; H, 5.08 %; N, 19.51 %. IR (KBr, cm^{-1}): 3282 (N-H), 3018 (C-H), 2949 (CH_2), 2811 (CH_2), 1564 (N-H), 1485 (C=C),1309, 1222, 1107 (C-O), 1022, 963, 864, 799, 736 (C-C). ^{1}H NMR ($CDCl_3$): δ (ppm), 8.98 (s, 2H, NH), 7.80-7.76 (s, 4H, Ar-H) 7.40-7.11 (dd, 8H, Ar-H), 4.23-4.15 (d, 16H, CH_2), 3.52-3.44 (d, 16H, CH_2). Uv-vis(DMF): λ_{max} (nm), (log ε): 323 (4.33), 644 (4.18), 682 (4.27), 745 (4.70), 775 (4.73). MALDI-TOF-MS m/z: Calc: 854.38; Found: [M+1H] = 855.12.

2.2.2.2 2(3),9(10),16(17),23(24)-Tetrakis-(morpholino)phthalocyanine (1b). Yield: 23 mg (12%). Anal calculated for $C_{48}H_{46}N_{12}O_4$, C, 67.43; H, 5.42; N, 19.66; found C 67.34 %; H, 5.09 %; N, 18.26 %. IR (KBr, cm^{-1}): 3280 (N-H), 3104 (C-H), 2899 (CH2), 2804 (CH2), 1557 (N-H), 1473 (C=C),1311, 1199, 1102 (C-O), 1032, 947, 804, 781, 731 (C-C). ^{1}H NMR ($CDCl_3$): δ (ppm), 9.02 (s, 2H, NH), 8.24- 8.18 (s, 4H, Ar-H), 7.78-7.62 (dd, 8H, Ar-H), 3.81-3.78 (d, 16H, CH_2),

3.28-3.24 (d, 16H, CH_2). Uv-vis(DMF): λ_{max} (nm), (log ε): 346 (4.42), 634 (4.38), 658 (4.41), 709 (4.58), 739 (4.62). MALDI-TOF-MS m/z: Calc: 854.38; Found: [M+2H] = 855.99.

2.3.3 General procedure for the synthesis of metallophthalocyanines (2a, 2b, 3a and 3b).

Compounds **4** or **5** (0.30 g, 1.4 mmol) and 0.35 mmol of metal salt (0.097 g $Zn(OAc)_2$ and 0.12 g $InCl_3$) were mixed in 3 ml of dry 1-pentanol and 0.1 ml DBU. The mixtures were stirred for 8 h at 138 °C. The products were precipitated with 1:1 methanol: H_2O, filtered and washed with acetonitrile. The products were further purified by column chromatography with silica gel and eluting with chloroform. All the complexes were soluble in $CHCl_3$, THF, DCM, DMF and DMSO.

1(4),8(11),15(18),22(25)-Tetrakis-(morpholino)phthalocyaninotozinc(II) (2a). Yield: 50 mg (23 %). Anal calculated for $C_{48}H_{44}N_{12}O_4Zn$, C, 62.78; H, 4.83; N, 18.30; found C 63.34 %; H, 4.09 %; N, 18.26 %. IR (KBr, cm^{-1}): 3189 (CH), 2910 (CH_2), 2837 (CH_2), 1601 (C=C),1309, 1220, 1094 (C-O), 1019, 946, 879, 810, 734 (C-C). ^{1}H NMR ($CDCl_3$): δ (ppm), 7.60 (s, 4H, Ar-H), 7.06-6.93 (m, 8H, Ar-H), 3.86-3.79 (d, 16H, CH_2), 3.41-3.29 (d,16H, CH_2). Uv-vis(DMSO): λ_{max} (nm), (log ε):340 (4.53), 682 (4.21), 747 (4.96). MALDI-TOF-MS m/z: Calc: 916.29; Found: [M] = 916.26.

2(3),9(10),16(17),23(24)-Tetrakis-(morpholino)phthalocyaninotozinc (2b). Yield: 93 mg (42.8 %). Anal calculated for $C_{48}H_{44}N_{12}O_4Zn$, C, 62.78; H, 4.83; N, 18.30; found C 62.94 %; H, 4.078 %; N, 18.81 %. IR (KBr, cm^{-1}): 3175 (CH), 2906 (CH_2), 2824 (CH_2), 1608 (C=C),1298, 1214, 1102 (C-O), 1020, 952, 869, 808, 729 (C-C). ^{1}H NMR ($CDCl_3$): δ (ppm), 7.71 (s, 4H, Ar-H), 6.92-6.72 (m, 8H, Ar-H), 4.18-3.49 (d, 16H, CH_2), 2.23-1.57 (d,16H, CH_2). Uv-vis(DMSO): λ_{max} (nm), (log ε): 364 (4.13), 644 (3.94), 717 (4.78). MALDI-TOF-MS m/z: Calc: 916.29; Found: [M] = 916.26.

1(4),8(11),15(18),22(25)-Tetrakis-(morpholino)phthalocyaninotoindium (3a). Yield: 43 mg (19.8 %). Anal calculated for $C_{48}H_{44}ClInN_{12}O_4$, C, 57.47; H, 4.42; N, 16.75; found C 56.83 %; H, 4.18 %; N, 16.32 %. IR (KBr, cm^{-1}): 3011 (C-H), 2948 (CH_2), 2849 (CH_2), 1493 (C=C),1330, 1225, 1104 (C-O), 1058, 985, 892, 777, 734 (C-C). ^{1}H NMR ($CDCl_3$): δ (ppm), 8.92 (s, 4H, Ar-H), 8.25-7.20 (m, 8H, Ar-H), 4.02-3.99 (d, 16H, CH_2), 3.27-3.18 (d,16H, CH_2). Uv-vis(DMSO): λ_{max} (nm), (log ε): 366 (4.08), 396 (3.94), 765 (4.71). MALDI-TOF-MS m/z: Calc: 1002.23; Found: [M] = 1002.49.

2(3),9(10),16(17),23(24)-Tetrakis-(morpholino)phthalocyaninotoindium (3b). Yield: 87 mg (40 %).. Anal calculated for $C_{48}H_{44}ClInN_{12}O_4$, C, 57.47; H, 4.42; N, 16.75; found C 57.27 %; H, 4.34 %; N, 16.02 %. IR (KBr, cm^{-1}): 3023 (C-H), 2909 (CH_2), 2823 (CH_2), 1510 (C=C),1396, 1198, 1108 (C-O), 1078, 962, 871, 762, 727 (C-C). ^{1}H NMR ($CDCl_3$): δ (ppm), 7.75 (s, 4H, Ar-H), 7.62-7.58 (m, 8H, Ar-H), 4.28-4.23 (d, 16H, CH_2), 3.93-3.88 (d,16H, CH_2). Uv-vis(DMSO): λ_{max} (nm), (log ε): 363 (3.98), 665 (3.75), 736 (4.68). MALDI-TOF-MS m/z: Calc: 1002.23; Found: [M] = 1002.89.

2.3.4 General procedure for the synthesis of phthalocyanines methylation (Q2a, Q2b, Q3a and Q3b).

Complexes **2a, 2b** (0.010 g, 0.011 mmol) or **3a and 3b** (0.010 g, 0.0099 mmol) and 5.05 mmol of dimethyl sulfate were mixed in 3 ml of dry DMF, followed by stirring for 4 h at 155 °C. The products were precipitated with acetone, filtered and washed with chloroform and diethyl ether. All the complexes were soluble in H_2O, DMF and DMSO.

1(4),8(11),15(18),22(25)-Tetrakis-(N-methylmorpholino)phthalocyaninotozinc(II) (Q2a). Yield: 3.4 mg (34 %). Anal calculated for $C_{52}H_{56}N_{12}O_{20}S_4Zn$, C, 45.83; H, 4.14; N, 12.33; S, 9.41; found C 43.14 %; H, 4.52 %; N, 11.55%; 9.72. IR (KBr, cm^{-1}): 3042 (CH), 2923 (CH_2), 1608

(C=C),1329, 1173, 1100 (C-O), 1041, 912, 850, 746 (C-C). ^{1}H NMR (D_2O): δ (ppm), 9.83 (s, 4H, Ar-H), 9.35-8.41 (m, 8H, Ar-H), 4.58-4.50 (m, 16H, CH_2), 4.31-4.25 (d,16H, CH_2), 2.18 (s, 12H, CH_3). Uv-vis(DMSO): λ_{max} (nm), (log ε):352 (4.84), 614 (4.53), 678 (5.20).

2(3),9(10),16(17),23(24)-Tetrakis-(N-methylmorpholino)phthalocyaninotozinc (Q2b). Yield: 5.2 mg (52 %). Anal calculated for $C_{52}H_{56}N_{12}O_{20}S_4Zn$, C, 45.83; H, 4.14; N, 12.33; S, 9.41; found C 44.78 %; H, 4.07 %; N, 11.92%; S, 9.35. IR (KBr, cm^{-1}): 3038 (CH), 2919 (CH_2), 1598 (C=C),1317, 1181, 1201 (C-O), 1001, 888, 832, 768 (C-C). ^{1}H NMR (D_2O): δ (ppm), 8.89 (s, 4H, Ar-H), 8.51-8.07 (m, 8H, Ar-H), 4.34-4.27 (m, 16H, CH_2), 4.08-4.02 (d,16H, CH_2), 3.88 (s, 12H, CH_3). Uv-vis(DMSO): λ_{max} (nm), (log ε):343 (4.98), 610 (4.64), 673 (5.33).

1(4),8(11),15(18),22(25)-Tetrakis-(N-methylmorpholino)phthalocyaninotoindium (Q3a). Yield: 2.7 mg (27 %). Anal calculated for $C_{52}H_{56}ClInN_{12}O_{20}S_4$, C, 43.15; H, 3.90; N, 11.61; S, 8.86; found C 44.03 %; H, 4.02 %; N, 11.89%; S, 9.06. IR (KBr, cm^{-1}): 3042 (CH), 2923 (CH_2), 1608 (C=C),1329, 1173, 1100 (C-O), 913, 861, 745 (C-C). ^{1}H NMR (D_2O): δ (ppm), 9.95 (s, 4H, Ar-H), 9.61-9.35 (m, 4H, Ar-H), 8.74-8.51 (m, 4H, Ar-H), 4.73-4.58 (m, 16H, CH_2), 4.31-4.27 (d,16H, CH_2), 3.64 (s, 12H, CH_3). Uv-vis(DMSO): λ_{max} (nm), (log ε):353 (4.51), 621 (4.17), 689 (4.90).

2(3),9(10),16(17),23(24)-Tetrakis-(N-methylmorpholino)phthalocyaninotoindium (Q3b). Yield: 2.7 mg (27 %). Anal calculated for $C_{52}H_{56}ClInN_{12}O_{20}S_4$, C, 43.15; H, 3.90; N, 11.61; S, 8.86; found C 43.65 %; H, 4.11 %; N, 11.73%; S, 9.07. IR (KBr, cm-1): 3039 (CH), 2927 (CH2), 1617 (C=C),1334, 1197, 1008 (C-O), 938, 817, 739 (C-C). 1H NMR (D_2O): δ (ppm), 9.63 (s, 4H, Ar-H), 9.45-9.27 (m, 4H, Ar-H), 9.03-8.78 (m, 4H, Ar-H), 4.52-4.41 (m, 16H, CH2), 4.38-4.26 (d,16H, CH_2), 3.22 (s, 12H, CH_3). Uv-vis(DMSO): λ_{max} (nm), (log ε):356 (4.72), 616 (4.46), 684 (5.11).

2.4 Photophysical and photochemical parameters

2.4.1 Fluorescence quantum yields (Φ_F)

Fluorescence quantum yields were determined by the comparative method (equation 1) using ZnPc as a standard (Φ_F^{Std} = 0.2 in DMSO) [**23**,**24**]

$$\Phi_F = \Phi_F^{Std} \frac{F\, A^{Std}\, n^2}{F^{Std} A\, (n^{Std})^2} \quad (1)$$

where F and F^{Std} are the areas under the emission curves of the sample and standard, respectively, A and A^{Std} are the absorbances of the sample and standard, respectively, and n and n^{Std} are the refractive indices of the solvents used for sample and standard, respectively. Absorbance at the excitation wavelength was ~ 0.05 in order to minimize inner filter effects. At least three independent experiments were performed for the quantum yield determinations. Both the sample and the standard were excited at the same relevant wavelength.

2.4.2. Triplet quantum yields (Φ_T)

The triplet quantum yields were determined in DMSO using a comparative method, and ZnPc as a standard in DMSO (Φ_T = 0.65 [**25**]), using Equations 2

$$\Phi_T = \Phi_T^{std} \frac{\Delta A_T\, \varepsilon_T^{std}}{\Delta A_T^{std} \varepsilon_T} \quad (2)$$

where Φ_T^{std} is the triplet quantum yield of the standard, ΔA_T and ΔA_T^{std} are the changes in the triplet state absorbances of the sample and the standard, respectively, ε_T and ε_T^{std} are the triplet state molar extinction coefficients for the sample and the standard, respectively

2.4.3. Singlet oxygen quantum yields (Φ_Δ)

Eq. 3 was employed for the determination of Φ_Δ employing ZnPc standard (Φ_Δ = 0.67 in DMSO) [**25**] and AlPcSmix (containing a mixture of differently sulfonated phthalocyanines, and synthesized as reported in literature [**26**]) in aqueous media (Φ_Δ =0.42) [**25**]. DPBF and ADMA were used as singlet oxygen quenchers in DMSO and aqueous media, respectively.

$$\Phi_\Delta = \Phi_\Delta^{\mathrm{Std}} \frac{W\ I_{abs}^{\mathrm{Std}}}{W^{\mathrm{Std}}\ I_{abs}} \quad (3)$$

where Φ_Δ^{Std} is the singlet oxygen quantum yield for the standard, W and W^{Std} are the DPBF and ADMA photobleaching rates in the presence of MPc derivatives under investigation and the standard, respectively, I_{abs} and I_{abs}^{Std} are the rates of light absorption by the MPc derivative and standard, respectively.

2.5 Antimicrobial studies

The nutrient broth and agar were prepared using manufacturer's specifications. Micro-organisms were cultured in broth, placed on a rotary shaker (~200 rpm) at 37°C until they reached an optical density of approximately 0.6. The resultant suspension was centrifuged at 3000 rpm for 15 min, the pellet was further washed thrice with PBS. A working solution was prepared by diluting to 1/1000 (10^6 colony forming unit (CFU)/mL. Photodynamic antimicrobial chemotherapy study was performed by dissolving the compounds in 0.2 % DMSO for all complexes (quaternized and unquaternized) and in water for quaternized which are completely soluble in water. For *S. aureus* and *C. albican*, 0.5 µM was prepared for each sample and for *E. coli* 2.5 µM was applied. In all the experiments, the bacterial/fungal suspensions were incubated in an oven equipped with a shaker for 30 min in the dark at 37°C. Then, half (2.5 mL) of the incubated bacterial/fungal suspensions were irradiated at the Q-

band maximum of the photosensitizers in 24 well plate, using the set-up described in supporting information and the other half kept in the dark. After irradiation, 100 µL samples were diluted with 900 µL PBS and were spotted on agar plates using micropipette. The plates were incubated at 37 ^{o}C for 24 h for both *S. aureus* and *E. coli* and for 48 h for *C. albican*. All the studies were conducted in triplicates.

3. Results and discussion

3.1 Synthesis and characterization

The synthetic route followed is shown in Scheme 1 for the unquaternized Pcs. The syntheses of phthalonitriles **4** and **5** were achieved through nucleophilic substitution between the nitro group of the 3/4-nitrophthalonitrile and the NH group from the morpholine at 100 °C in dry DMF with Na_2CO_3 as a base catalyst for 18 h under N_2 gas. IR spectra confirmed the formation of the morpholiniphthalonitriles (**4** or **5**) where there was a presence of two sharp -CH_2 bands at 2907, 2869 and 2909, 2864 cm^{-1}, as well a strong -C≡N band at 2218 and 2221 cm^{-1} for **4** and **5**, respectively. The cyclotetramerization of **4** or **5** was performed in the presence of DBU and dry DMF producing the metal-free phthalocyanines **1a** or **1b** and with the addition of metal salts; $Zn(OAc)_2$, $InCl_3$ for **2a, 2b, 3a** and **3b**. The metallophthalocyanines were further quaternized using dimethyl sulfate (Scheme 2). IR spectra of the all Pcs showed the disappearance of the -C≡N band of the phthalonitriles on formation of the Pcs, with H_2Pcs (**1a** and **1b**) showing an additional –NH peak at 3282 and 3280 cm^{-1}, respectively. The compounds were further characterized using elemental analysis, ^{1}H NMR, MALDI-TOF mass spectroscopy and UV-vis. The results obtained were comparable with the proposed structures. ^{1}H NMR were recorded in deuterated $CDCl_3$ for all the unquaternized compounds and D_2O for the quaternized compounds which gave the expected signals. For all the phthalocyanine

complexes, the aromatic protons appeared between 6.72 and 9.95 ppm, and the CH_2 protons between 1.59 and 4.58 ppm. The quaternized compounds had an additional sharp singlet upfield (δ = 3.88-2.18 ppm) from the additional –CH_3 protons. Compound **1a** and **1b**) had an additional singlet signal at 8.98 and 9.02 ppm, respectively, attributed to the presence of –NH. In mass spectroscopy, all the proposed structures were obtained with peaks at 855.15 as [M+1H], 916.26 [M] and 1002.46 [M] for **1a**, **2a** and **3a**, respectively.

3.2 Ground state electronic absorption properties

The UV-Vis spectra of complexes **2a, 2b, 3a, 3b, Q2a, Q2b, Q3a, Q3b**) showed a single sharp Q band typical of monomeric phthalocyanines [**27**]. The UV-Vis of the H_2Pcs **1a** and **1b** (Fig. 1(i)) showed characteristic split Q band at 775 and 745 nm for **1a** and 739 and 709 nm in DMF for **1b** (Table 1), respectively, confirming the structure to be of D_{2h} symmetry. However, Compounds **1a** and **1b** showed a single Q bands in DMSO (Fig. 1, insert), suggesting deprotonation of the inner pyrrolic H atoms in the Pc core and thus, symmetry change from D_{2h} to D_{4h} occurs due to basicity of these solvents [**28**].

Compounds **2a** and **2b** (Fig. 1(ii)) showed a Q-band at 747 and 717 nm and compounds **3a** and **3b** (Fig. 1(iii)) showed the characteristic Q-band peak at 765 and 736 nm in DMSO (Table 1). The non-peripherally substituted compound **1a**, **2a** and **3a** were red shifted when compared to the peripherally substituted compounds **1b, 2b** and **3b**. This large-scale red shift can be attributed to the linear combinations of the atomic orbitals coefficients at the non-peripheral positions of the highest occupied molecular orbital (HOMO) being greater than that of peripheral positions [**29**]. As a result, the HOMO level is destabilized more at the non-peripheral position that it is at the peripheral position, resulting in the red shifting of the Q band in the former.

For all Pcs there was an additional peak observed between 400 nm and 500 nm attributed to charge transfer [**30**]. The Pcs were dissolved in THF, DCM and DMSO to examine the solvent effect as well the aggregation behaviour of the newly synthesized Pcs, Fig. 2. All Pcs show no aggregation in the above mentioned solvents. Lambert-Beer's Law was obeyed in the concentration range 5.5×10^{-6} to 3.5×10^{-5} mol/L (Fig. S1A for **2b** used as an example) in DMSO. With increase polarity of the solvent (THF < DCM < DMSO) there was a spectral shift as shown in Fig. 2. The MPcs upon quaternization became blue shifted (Fig. 3) in DMSO and in aqueous media containing 0.2% DMSO, Table 1. This is due to the lowering of the electron donating ability of the nitrogen groups upon quaternization. There were slight red shifts in the Q band maxima for the quaternized in aqueous media compared to in DMSO, Table 1, due to the increase in polarity. Spectra were recorded in water containing 0.2% DMSO since this was the media used for bacterial work. Phthalocyanines are known to aggregate in aqueous solution [**31**], mainly through the formation of the so called H aggregates. This type of aggregation is evidenced by broadening and splitting of the Q band, with the high energy band being due to the aggregate and the low energy band to the monomer. The quaternized derivatives (**Q2a**, **Q2b**, **Q3a** and **Q3b**) were soluble in aqueous solution and showed no sign of aggregation in water alone or with 0.2% DMSO (Fig. 3 for **Q3b** used as an example for water plus 0.2% DMSO). The spectra in water with or without 0.2% DMSO were similar. Water solubility and lack of aggregation are imperative for the PACT applications. Lambert-Beer's Law was obeyed in water in the concentration ranging from 6.23×10^{-6} to 8.90×10^{-6} mol/L (Fig. S1B for **Q2b** as an example). However, the neutral unquaternized derivatives (using complex **3b** as an example in Fig. 3), were highly aggregated as evidenced by the split Q band. This will affect their PACT activity as will be discussed below.

3.3 Physicochemical parameters

3.3.1. Fluorescence quantum yields and lifetimes

The fluorescence absorption, excitation, and emission spectra of **2b** is shown in Fig. 4. There was splitting of the excitation spectrum showing change in symmetry following excitation. Both indium Pcs exhibited very low intensity due to the heavy atomic effect of the central metal hence not shown.

The fluorescence quantum yields were performed in DMSO and aqueous media using ZnPc and AlPcSmix, respectively, as standards. Generally, all compounds (**1a, 1b, 2a, 2b, 3a and 3b**) had a weak fluorescence emissions and low Φ_F values common to morpholine containing Pcs [**32**].

Compounds **1a** and **1b** showed larger Φ_F values of 0.08 and 0.09 respectively, compared to the metalled Pcs. The presence of metals encourage the population of the triplet via intersystem crossing for complexes **2a,b** and **3a,b.** The quaternized compounds **Q2a** and **Q2b,** had an intense fluorescence emission, with higher Φ_F values of 0.19 and 0.24, respectively. The Φ_F values for the quaternized complexes **3** are lower than for quaternized complexes **2**, since In is heavier than Zn, hence the former results in enhanced heavy atom effect. The Φ_F values in water decreased to 0.09, 0.11 for **Q2a** and **Q2b**. For **Q3a** and **Q3b** the values were below 0.01 in aqueous media due to the quenching effect of water.

Time-correlated single photon counting was used to determine the fluorescence lifetime (Table 1). All Pcs showed mono-exponential decay shown in Fig. 5 with their corresponding residual graph in DMSO. The metal-free Pc **1a** and **1b** showed higher ns lifetimes of 2.08 and 5.48 due to the absence of a metal, while the metalled Pc showed a general decrease in

lifetimes. All the peripheral Pcs had a higher lifetime compared to the non-peripheral Pcs highlighting the effects of substituent position.

3.3.2. Triplet quantum yields and lifetimes

Laser flash photolysis was used to determine the triplet quantum yields and triplet lifetimes in DMSO using ZnPc as a standard. Transient absorption of the ZnPc (Fig. 6) (following excitation at 682 nm for **Q3a**, 679 nm for **Q3b**, 680 nm for **Q2a** and 670 for **Q2b**) showed a broad T_1- T_n triplet absorption peak at 480 nm [**33**]. The unquaternized complexes (**1a, 1b**, **2a, 2b, 3a, 3b**) gave a very weak signal. It has been shown before that nitrogen containing substituents bound directly to the Pcs ring quench the triplet state [**34**], hence no triplet quantum yield values in Table 1. In contrast, the introduction of the methyl groups to the nitrogen atoms improved the signal (Fig. 6) with the Φ_T values of **Q2a**, **Q2b**, **Q3a**, **Q3b** being 0.71, 0.66, 0.92, 0.87, respectively, Table 1. The non-peripheral Pcs had higher values than peripheral Pcs, corresponding to the low fluorescence quantum yields of the former. The heavier central atom, indium yielded a greater conversion to the triplet state than the corresponding zinc complexes.

Triplet state lifetimes (τ_T) were studied to confirm the population of the triplet state, the decay curve (Fig. 6, insert) showed the expected mono-exponential decay with heavy indium Pcs (**Q3a** and **Q3b**) with lower lifetime of 76 and 92 μs when compared to 112 and 292 μs of **Q2a** and **Q2b**, respectively. The peripheral Pcs had longer lifetime compared to their non-peripheral counterparts due to the reasons stated above, corresponding to the large Φ_T values. Efficient spin orbit coupling (heavy atom effect) is known to result in shortening of triplet lifetimes and increase in triplet quantum yields [**35**]. There were no signals in aqueous media.

3.3.3. Photostability and singlet oxygen quantum yields

Prior to their use for PACT, the photostabilities of the compounds were evaluated. The spectral changes of each compound were observed in DMSO after 30 seconds of irradiating with light. Predominantly, all Pcs showed no to low significant changes upon the introduction of light over time as shown in Fig. S2 (ESI). Both the Q-band and the B-band spectra maintain their original shape and intensity, therefore our compounds were stable. Singlet oxygen quantum yields (Φ_Δ) of the metal-free and metallated Pcs were determined in DMSO using 1,3-diphenylisobenzofuran (DPBF) and anthracene-9,10-bis-methylmalonate (ADMA in water containing 0.2% DMSO) as a quenchers. The solutions were irradiated in 10 seconds intervals. A similar trend to the photostability studies was observed where there was a minimal Q-band change, Fig. 7. The degradations of the DPBF band at 417 nm and ADMA at 380 nm were monitored (Fig. 7). Akin to the previous properties, the indium Pcs generated the highest values of Φ_Δ, 0.68, 0.63, 0.66 and 0.62 for **3a**, **3b, Q3a** and **Q3b** compared to 0.54, 0.47, 0.58 and 0.50 of **2a**, **2b, Q2a** and **Q2b**, respectively in DMSO. The importance of metalation was evident as the metal-free Pcs **1a** and **1b** illustrated considerably lower Φ_Δ than the metallated Pcs due to the absence of a heavy metal. The Φ_Δ values decrease in water since water is a known quencher [**36**]. This could also be due to the fact that oxygen has higher solubility in many organic solvents used in this study compared to water [**37**], which could be responsible for low singlet oxygen generation in water. Non-peripheral substituted Pcs (**1a**, **2a, 3a, Q2a** and **Q3a**) had larger Φ_Δ values compared to the corresponding peripherally substituted (**1b**, **2b**, **3b, Q2b** and **Q3b**) corresponding to the higher triplet quantum yields for **Q2a** and **Q3a** compared to respective **Q2b** and **Q3b**.

3.4 Bacterial studies

The antimicrobial activities of **2a, 2b, 3a, 3b, Q2a, Q2b, Q3a** and **Q3b** were studied against gram positive *S. aureus,* gram negative *E. coli* and fungi *C. albican*. The phthalocyanines were dissolved in 0.2 % DMSO (diluted with PBS) for all complexes and in water only for the quaternized derivatives. A control using the same amount of DMSO in the culture was assessed and the organic solvent had negligible effects hence used (Fig. 8(i)). For all Pcs the optimum concentration was determined to be 0.5 µM for *S. aureus* and *C. albican* studies and 2.5 µM for *E. coli.* The bacterial suspension of 10^6 CFU/mL was used for all micro-organisms. Log reductions and reduction percentage were used to quantify the results, Fig. 8, Table 2. The cationic Pcs (**Q2a, Q2b, Q3a and Q3b**) had higher log reductions (9.90, 9.84, 9.92, 9.87) than the neutral derivatives (1.17, 1.36, 1.03, 1.21) against *E. coli* in aqueous media containing 0.2% DMSO. The cationic Pcs are hydrophilic which encourages interaction between the dyes and cytoplasm of the micro-organisms. For *C. albican*, the log reduction values for neutral Pcs were below 2. But when evaluating the results using percentage reduction of the viable cells (Fig. 8 (ii)), there was an observed increase of the reduction percentage for **2a, 2b, 3a, 3b** of 60.2%, 68.5 %, 35.6 %, 40.3 % for *C. albican,* compared to 32.8 %, 48.6 %, 27.1%, 30.4 % for *S. aureus*, respectively. This increase of the hydrophobic compounds was due to the antifungal property of the morpholine group. Morpholines are known ergosterol synthesis inhibitors, which is a hormone that stimulates the growth in fungi [**38**]. Moreover, the methylated Pcs took less than 45 min to reduce *C. albican* colonies, which is faster than *E. coli and S. aureus.* Generally, there was a moderate difference between the non-peripheral, peripheral, zinc and indium Pcs. Additionally, the solubility improved the engagement between the dye and the micro-organism hence the cationic compounds had very high log reductions. The inability to penetrating or interacting with cell limits the singlet oxygen's potential to terminate the micro-organism. The low log reduction for the unquartenized

phthalocyanines could be a result of aggregation (shown in Fig. 3), which would affect the penetration of dyes into the cell wall and membrane [**39**]. The log reduction values in the presence of DMSO are not too different from the values in aqueous solution only for the quaternized derivatives, Table 2.

4. Conclusions

The syntheses of novel non-peripherally and peripherally morpholine tetra-substituted metal free phthalocyanines, Zn(II), In(III) and the quaternized metallated Pcs are presented. The compounds were characterized using various methods such as elemental analysis, infrared, ultra-violet visible, ^{1}H nuclear magnetic resonance and MALDI-TOF spectroscopy. Generally, the Pcs were soluble in most organic solvents such as DCM, THF, chloroform, DMF and DMSO. The photophysical and photochemical parameters were studied in DMSO and singlet oxygen quantum yields in water for the quaternized derivatives. The non-peripherally substituted Pcs showed red shifted spectra when compared to the peripheral Pcs, with the H_2Pcs showing a split Q-band in DMF. The fluorescence quantum yield values decreased with the introduction of metals and increased with quaternization. In turn, the singlet oxygen quantum yields were significantly higher for the indium Pcs than the zinc and metal-free Pcs. All the non-peripheral Pcs had higher Φ_Δ values compared to the peripheral value in DMSO. The Φ_Δ values of these

compounds range from 0.20 to 0.68 in DMSO. The Pcs were applied for PACT of *E. coli*, *S. aureus* and *C. albican* where the cationic Pcs were far superior than the neutral Pcs.

Acknowledgements

This work was supported by the Department of Science and Technology (DST) Innovation and National Research Foundation (NRF), South Africa through DST/NRF South African Research Chairs Initiative for Professor of Medicinal Chemistry and Nanotechnology (UID 62620) as well as Rhodes University. This work was also partially supported by a bilateral program between the Japan Society for the Promotion of Science (JSPS) and NRF of South Africa (uid: 92425), JSPS KAKENHI grant numbers 15H00910 and18K05076.

References

1. A. Ozel, B. Barut, U. Demirbas, Z. Biyiklioglu, nvestigation of DNA binding, DNA photocleavage, topoisomerase I inhibition and antioxidant activities of water soluble titanium(IV) phthalocyanine compounds, J. Photochem. Photobiol. B 157 (2016) 32-38.
2. N. Masilela, P. Kleyi, Z. Tshentu, G. Priniotakis, P. Westbroek, T. Nyokong, Photodynamic inactivation of Staphylococcus aureus using low symmetrically substituted phthalocyanines supported on a polystyrene polymer fiber, Dyes Pigm. 96 (2013) 500–508.
3. L. Xodo, S. Cogoi, V. Rapozzi, Photosensitizers binding to nucleic acids as anticancer agents, Future Med. Chem. 8 (2016) 179-194.
4. C.C. Jayme, I.R. Calori, A.C. Tedesco, Spectroscopic analysis of aluminium chloride phthalocyanine in binary water/ethanol systems for the design of a new drug delivery system for photodynamic therapy cancer treatment, Spectrochim. Acta A 153 (2016) 178–183.
5. N. Nombona, K. Maduray, E. Antunes, A. Karsten, T. Nyokong, Synthesis of phthalocyanine conjugates with gold nanoparticles and liposomes for photodynamic therapy, J. Photochem. Photobiol. B 107 (2012) 35–44.
6. O. M. Bankole, T. Nyokong, Mercaptopyridine-substituted indium, zinc, and metal-free phthalocyanines: nonlinear optical studies in solution and on polymer matrices, Coord. Chem. 68 (2015) 3727-3740.

7. L. K. Kumawat, N. Mergu, A. K. Singh, V. K. Gupta, A novel optical sensor for copper ions based on phthalocyanine tetrasulfonic acid, Sens Actuators B. 212 (2015) 389-394.
8. J. Xu, Y. Wang, Q. Chen, Y. Lin, H. Shan, V. A. L. Roy, Z. Xu, Enhanced lifetime of organic light-emitting diodes using soluble tetraalkyl-substituted copper phthalocyanines as anode buffer layers, J. Mater. Chem. C. 4 (2016) 7377-7382.
9. M. Han, X. Zhang, X. Zhang, C. Liao, B. Zhu, Q. Li, Azo-coupled zinc phthalocyanines: Towards broad absorption and application in dye-sensitized solar cells, Polyhedron 85 (2015) 864-873.
10. R. O. Ogbodu, J. L. Limson, E. Prinsloo, T. Nyokong, Photophysical properties and photodynamic therapy effect of zinc phthalocyanine-spermine-single walled carbon nanotube conjugate on MCF-7 breast cancer cell line, Synth Met. 204 (2015) 122-132.
11. A. Sindelo, O. L. Osifeko, T. Nyokong, Synthesis, photophysicochemical and photodynamic antimicrobial chemotherapy studies of indium pyridyl phthalocyanines: Charge versus bridging atom, Inorg. Chim. Acta. 476 (2018) 68-76.
12. K. E. Sekhosana, E. Amuhaya, T. Nyokong, Nanosecond nonlinear optical limiting properties of new trinuclear lanthanide phthalocyanines in solution and as thin films, Polyhedron 85 (2015) 347-354.
13. K. P. Priyanka, S. Sankararaman, K. M. Balakrishna, T. Varghese, Enhanced visible light photocatalysis using TiO_2/phthalocyanine nanocomposites for the degradation of selected industrial dyes, J. Alloys Compd. 720 (2017) 541-549.
14. J. Chen, Z. Chen, Y. Zheng, S. Zhou, J. Wang, N. Chen, J. Huang, F. Yan, M. Huang, Substituted zinc phthalocyanine as an antimicrobial photosensitizer for periodontitis

treatment, J. Porphyr. Phthalocyanines. 15 (2011) 293-299. https://doi.org/10.1142/S1088424611003276

15. M. Managa, E.K. Amuhaya, T. Nyokong, Photodynamic antimicrobial chemotherapy activity of (5,10,15,20-tetrakis(4-(4-carboxyphenycarbonoimidoyl)phenyl)porphyrinato) chloro gallium(III), Spectrochim. Acta. A. Mol. Biomol. Spectrosc. 151 (2015) 867-874. https://doi.org/10.1016/j.saa.2015.06.088
16. M. Wainwright, Photodynamic antimicrobial chemotherapy (PACT), J. Antimicrob. Chemother. 42 (1998) 13-28.
17. V. Mantareva, I. Angelov, D. Wöhrle, V. Dogandjiska, R. Dimitrov, V. Kussovski, Water-soluble phthalocyanine complexes of Ga(III) and In(III) in the photodynamic inactivation of pathogenic fungus, Proc. of SPIE. 7747 (2011)774712-9.
18. O.L. Osifeko, M. Durmuş, T. Nyokong, Physicochemical and photodynamic antimicrobial chemotherapy studies of mono- and tetra-pyridyloxy substituted indium(III) phthalocyanines, J. Photochem. Photobiol. A Chem. 301 (2015) 47-54. https://doi.org/10.1016/j.jphotochem.2014.12.011
19. T.J. Beveridge, Structures of gram-negative cell walls and their derived membrane vesicles, J. Bacteriol. 181 (1999) 4725-4733.
20. Hakan Bektaş, Şule Ceylan, Neslihan Demirbaş, Şengül Alpay-Karaoğlu, Bahar Bilgin Sökmen, Antimicrobial and antiurease activities of newly synthesized morpholine derivatives containing an azole nucleus, Med Chem Res. 2013 Aug; 22(8): 3629–3639.

21. J. Britton, E. Antunes, Tebello Nyokong, Fluorescence quenching and energy transfer in conjugates of quantum dots with zinc and indium tetraamino phthalocyanines, J. Photochem. Photobiol. A 210 (2010) 1-7.

22. A. B. Sorokin, Phthalocyanine Metal Complexes in Catalysis, Chem. Rev. 113 (2013) 8152–8191.

23. S. Fery-Forgues, D. Lavabre, Are fluorescence quantum yields so tricky to measure? A Demonstration using familiar stationery products, J. Chem. Educ., 76 (1999)1260-1264.

24. A. Ogunsipe, J. Chen, T. Nyokong, , Photophysical and photochemical studies of zinc(II) phthalocyanine derivatives—effects of substituents and solvents, New J. Chem., 28 (2004) 822-827.

25. T. Nyokong, E. Antunes, Photochemical and photophysical properties of metallophthalocyanines, Eds: K. Kadish, K. Smith, R. Guilard, The handbook of pophyrin science, vol. 7, 2010, Academic Press, New York.

26. M. Ambroz, A. Beeby, A.J. McRobert, M.S.C. Simpson, R.K. Svensen, D. Phillips, Preparative, analytical and fluorescence spectroscopic studies of sulphonated aluminium phthalocyanine photosensitizers, J. Photochem, Photobiol. B: Biol. 9 (1991) 87-95. doi.org/10.1016/1011-1344(91)80006-4

27. H. Y. Yenilmez, I. Özçeşmeci, A. Okur, A. Gül, Synthesis and characterization of metal-free and metallo phthalocyanines with four pendant naphthoxy-substituents, Polyhedron 23 (2004) 787-791.

28. M.J. Stillman, T. Nyokong In: Eds. C. C. Leznoff and A. B. P. Lever Phthalocyanines: Properties and applications. New York: VCH Publishers; (1989) Ch 3.

29. T. Soganci, Y. Baygu, N. Kabay, Y. Gök, M. Ak, Comparative investigation of peripheral and nonperipheral zinc phthalocyanine-based polycarbazoles in terms of optical, electrical, and sensing properties, ACS Appl. Mater. Interfaces 2018, 10, 21654−21665

30. X-F. Zhang, X. Li, L. Niu, L. Sun, L. Liu, Charge transfer photophysics of tetra(α-amino) zinc phthalocyanine, J. Fluoresc. 19 (2009) 947-954.

31. N. Kobayashi, R. Higashi, K. Ishii, K. Hatsusaka, K. Ohta, Aggregation, Complexation with Guest Molecules, and Mesomorphism of Amphiphilic Phthalocyanines Having Four- or Eight Tri(ethylene oxide) Chains, Bull. Chem. Soc. Jpn. 72 (1999) 1263–1271.

32. Y.-J. Zhu, J.-D Huang, X.-J. Jiang, J.-C. Sun, Novel silicon phthalocyanines axially modified by morpholine: Synthesis, complexation with serum protein and *in vitro* photodynamic activity, Inorg. Chem. Commun. 9 (2006) 473-477.

33. K. Ishii, Functional singlet oxygen generators based on phthalocyanines, Coord. Chem. Rev. 256 (2012) 1556–1568.

34. X. F. Zhang, Y. Di, F. Zhang, Photoinduced single and double-electron transfer in a photosynthetic model consisting of one-acceptor with four equally linked donor (D_4-A). J. Photochem. Photobiol. A, 203 (2009) 216-221.

35. J.R. Darwent, P. Douglas, A. Harriman, G. Porter, M.C. Richoux, Metal phthalocyanines and porphyrins as photosensitizers for reduction of water to hydrogen, Coord. Chem. Rev. 44 (1982) 83–126.

36. C. Tanielian, C. Wolff, M. Esch, Singlet oxygen production in water: Aggregation and charge-transfer effects, J. Phys. Chem. 100 (1996) 6555–6560.

37. H. Ramesh, T. Mayr, M. Hobisch, S. Borisov, I. Klimant, U. Krühne, J. M. Woodley Measurement of oxygen transfer from air into organic solvents, J. Chem. Technol. Biotechnol. 91 (2016) 832–836.

38. M. K. Kathiravan, A. B. Salake, A. S. Chothe , P. B. Dudhe, R. P. Watode, M. S. Mukta, S. Gadhwe, The biology and chemistry of antifungal agents: A review, Bioorg. Med. Chem. 20 (2012) 5678–5698.

39. D. Liu, L. Li, J. Chen, Z. Chen, L. Jiang, C. Yuan, M. Huang, Dissociation of zinc phthalocyanine aggregation on bacterial surface is key for photodynamic antimicrobial effect, J. Porphyrins and Phthalocyanines 22(2018) 925–934.

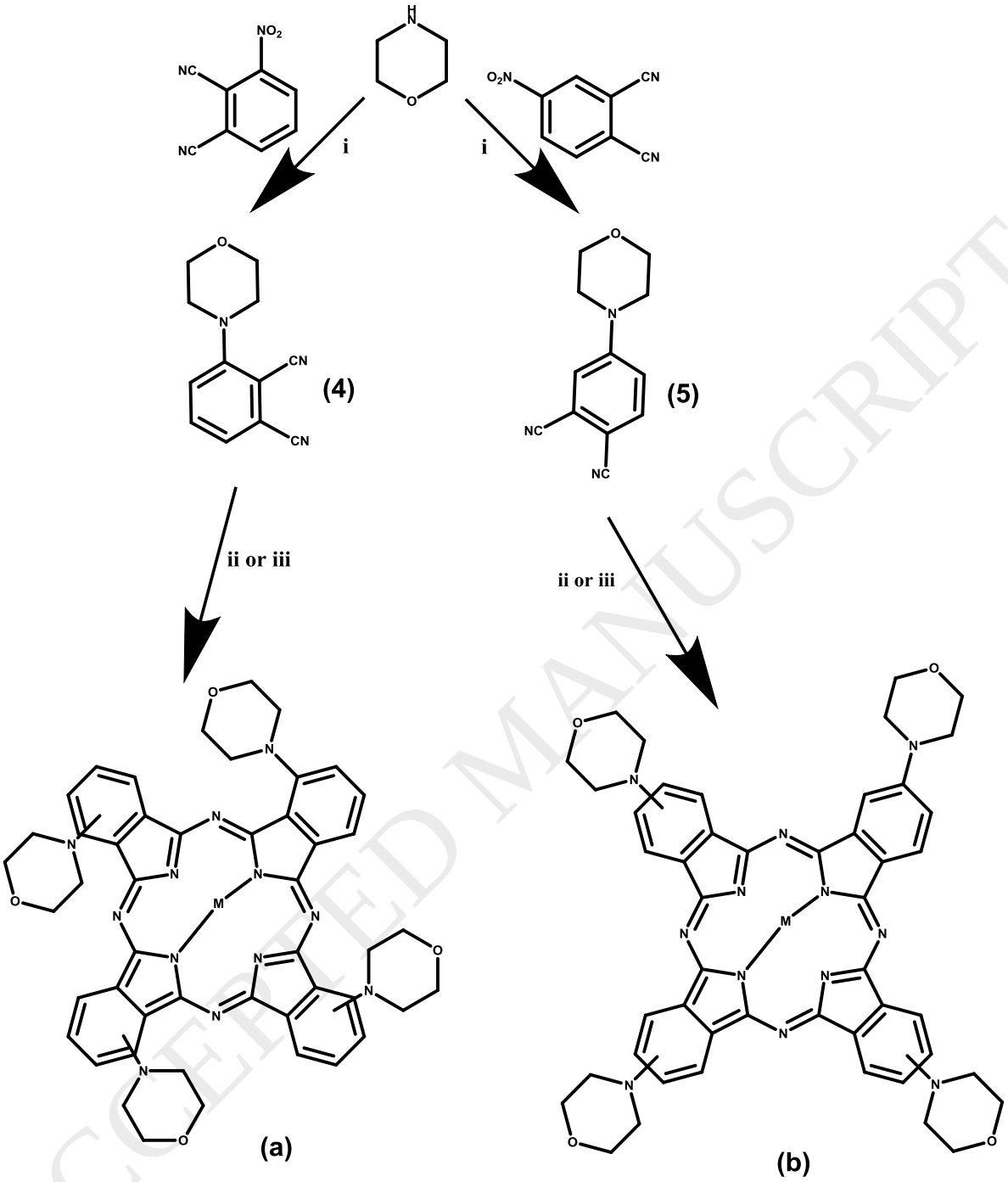

Scheme 1: Synthetic route of phthalonitriles (**a** or **b**) using (i) N_2, dry DMF, Na_2CO_3, 18 h and phthalocyanines (**1a – 3b**), (ii) N_2, n-pentanol, DBU, 138 °C, 8h; (iii) N_2, $Zn(OAc)_2$ or n-pentanol, DBU, 138 °C, 8h.

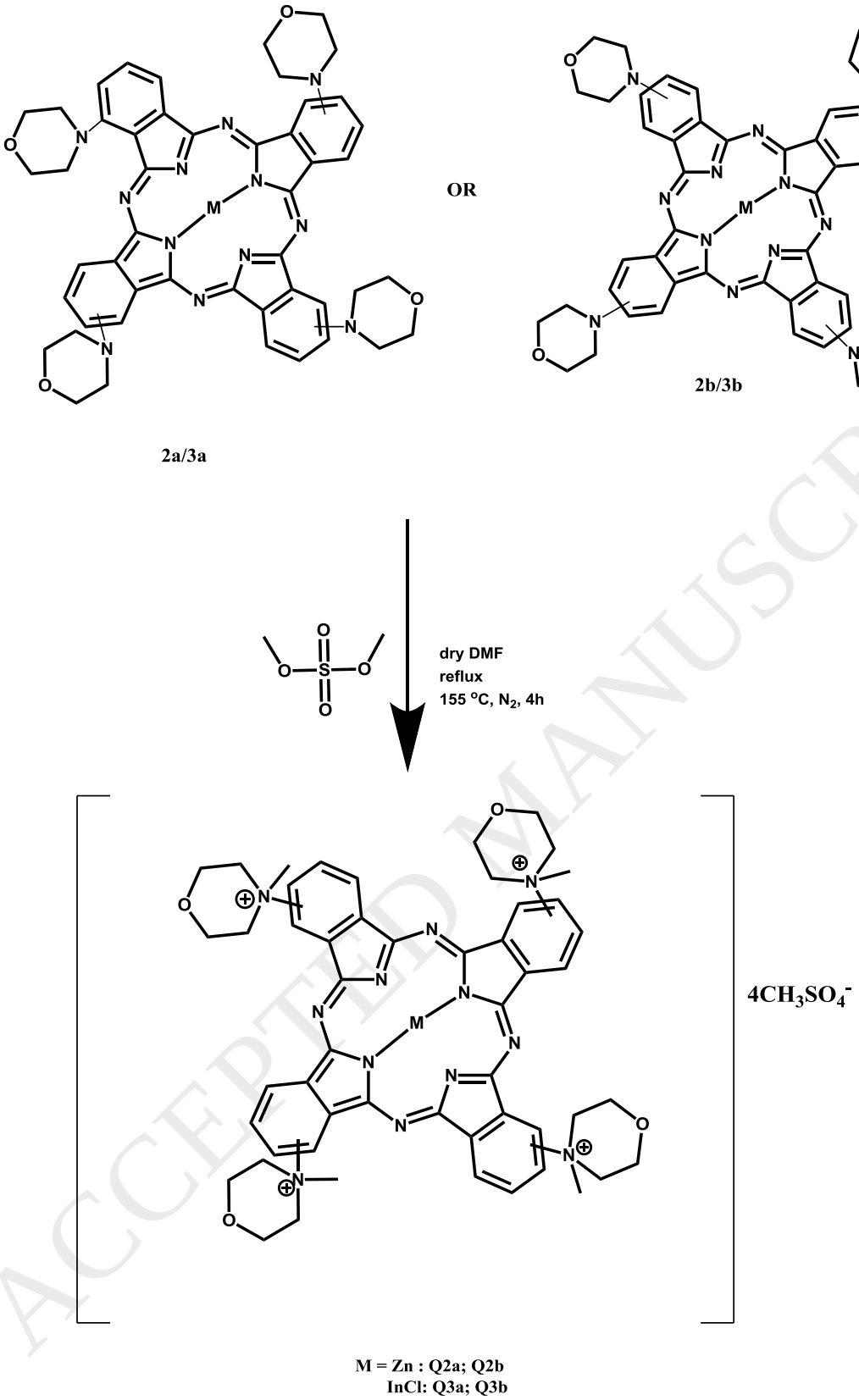

Scheme 2: Synthetic route of the quaternized phthalocyanines using dimethyl sulfate, dry DMF, 155 ^{o}C, 4 h.

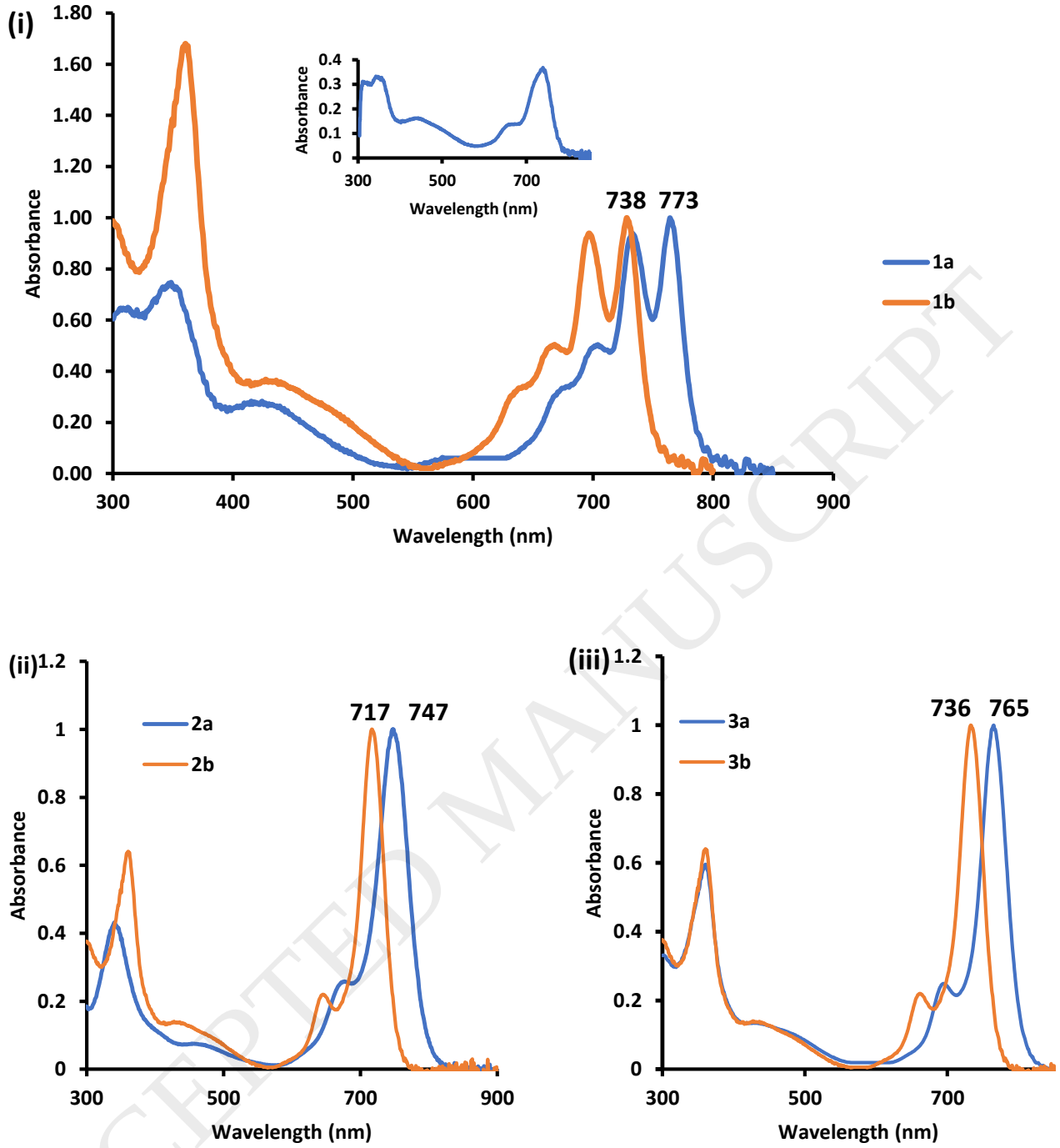

Figure 1: UV-vis spectra of i) **1a** and **1b** in DMF; ii) **2a** and **2b**; iii) **3a** and **3b** in DMSO with the Q bands labelled. The insert in (i) is the spectrum of **1b** in DMSO.

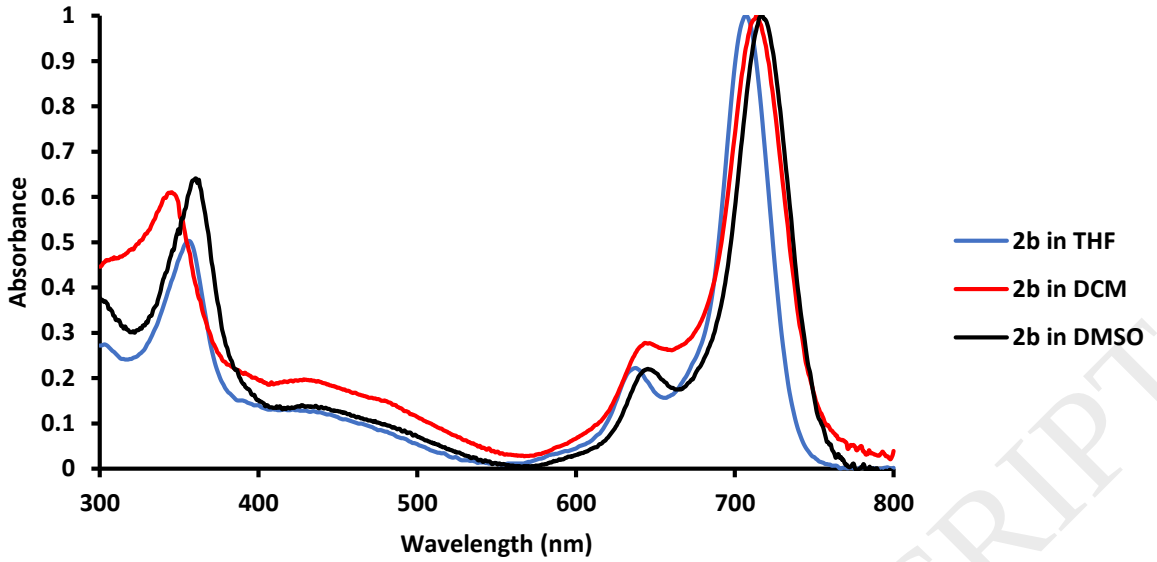

Figure 2: UV-Vis spectra of **2b** in different solvents.

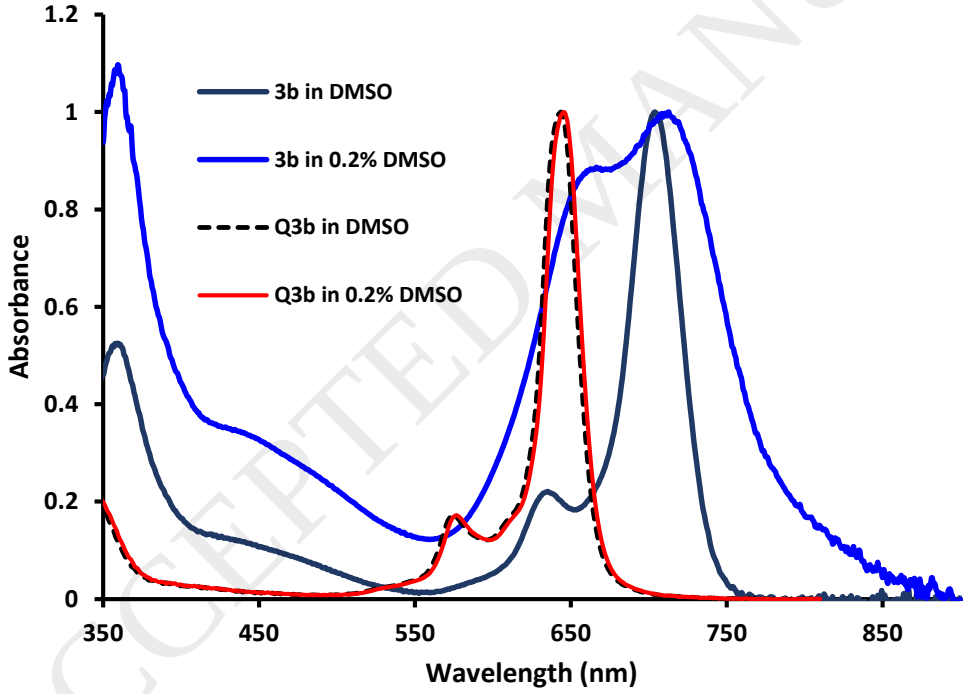

Figure 3: Absorption spectra of **3b** and **Q3b** in DMSO and **3b** and **Q3b** in 0.2% DMSO in water.

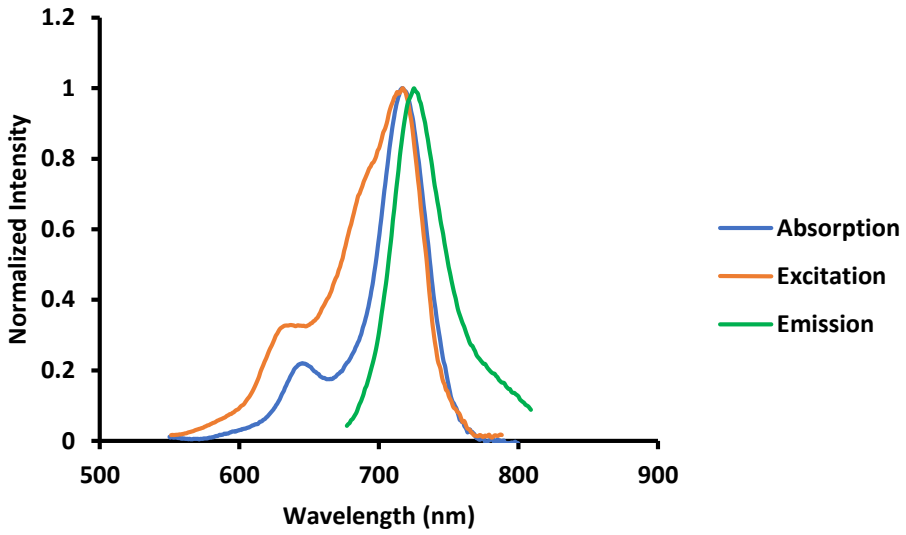

Figure 4: Absorption, excitation and emission spectra in DMSO of **2b** at the excitation wavelength of 725 nm.

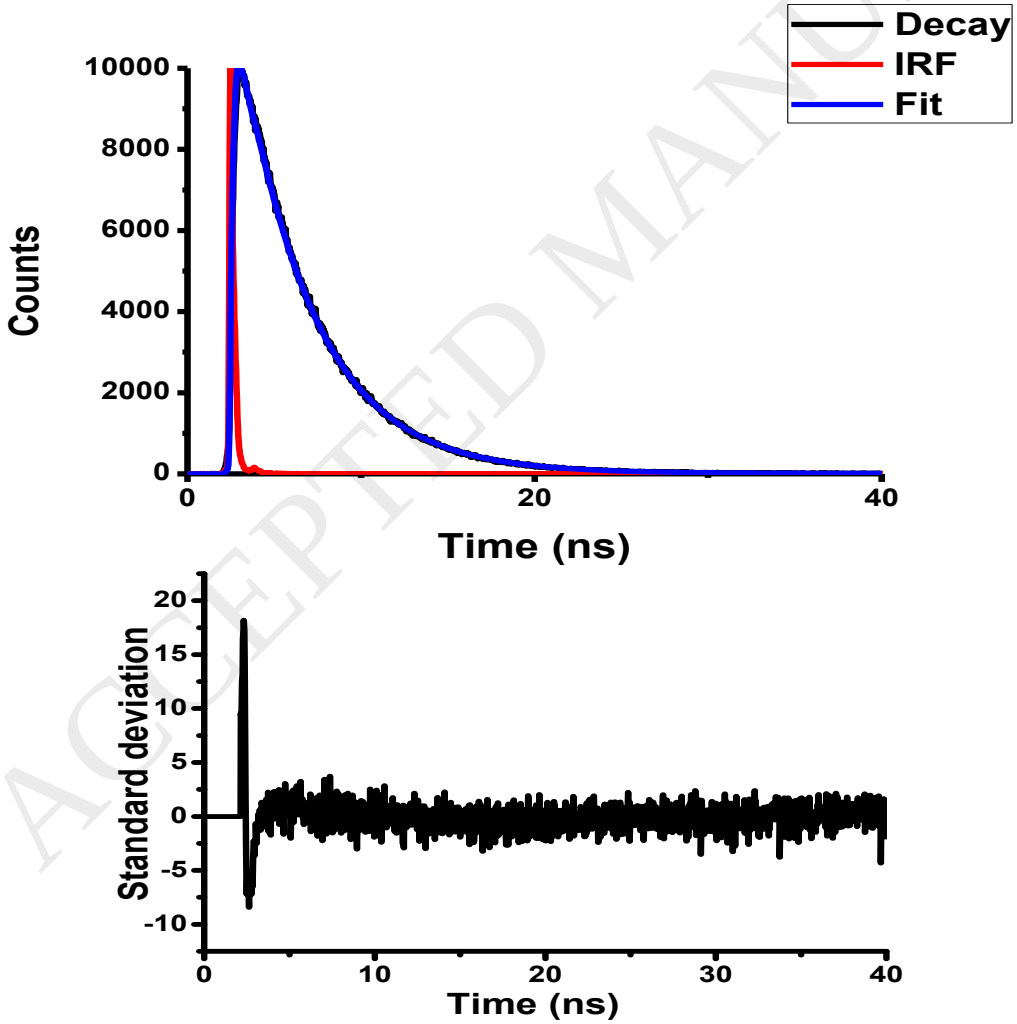

Figure 5: Time-correlated single photon counting decay and residual for **2b** and at the excitation wavelength of 725 nm. IRF = instrument response function. χ^2 = 0.998

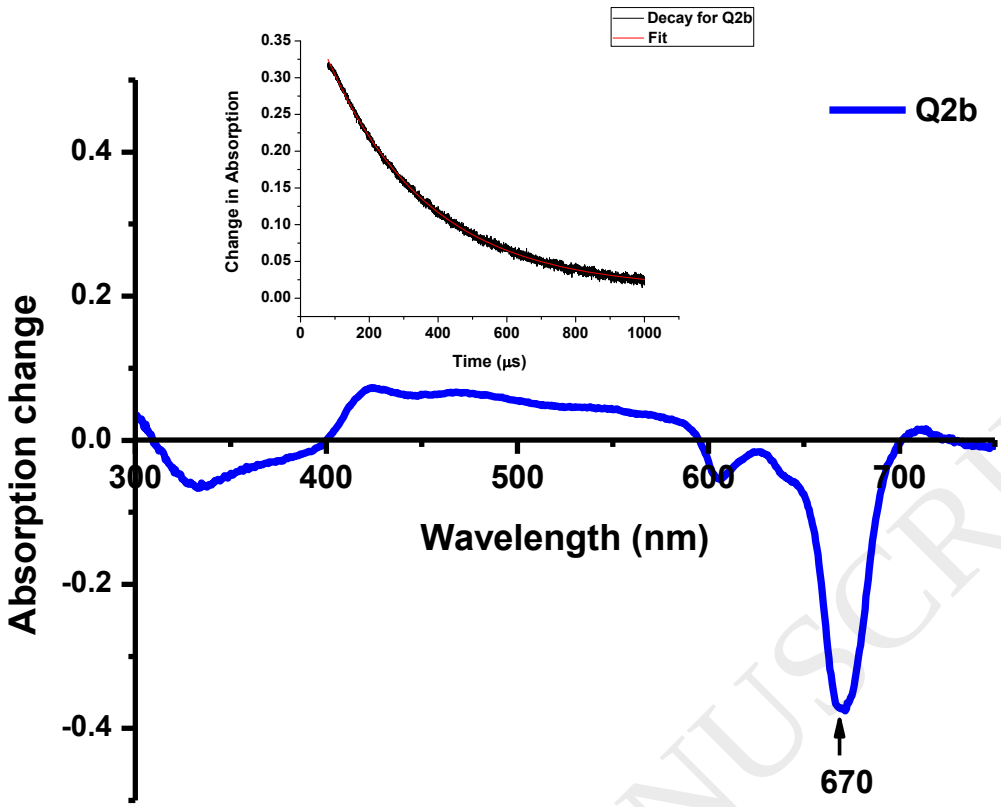

Figure 6: Transient absorption curve for **Q2b** in DMSO**.** The insert is the triplet decay curve for **Q2b**. Excitation wavelength = 670 nm.

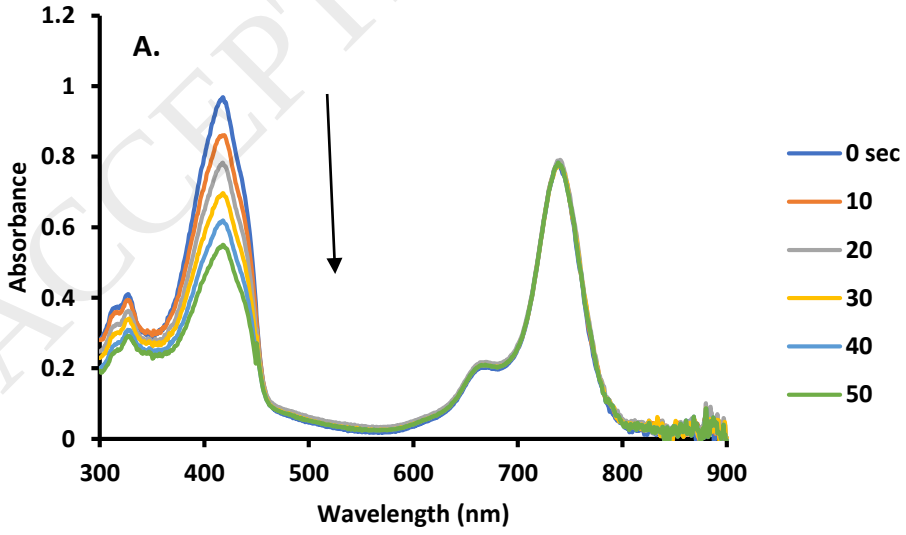

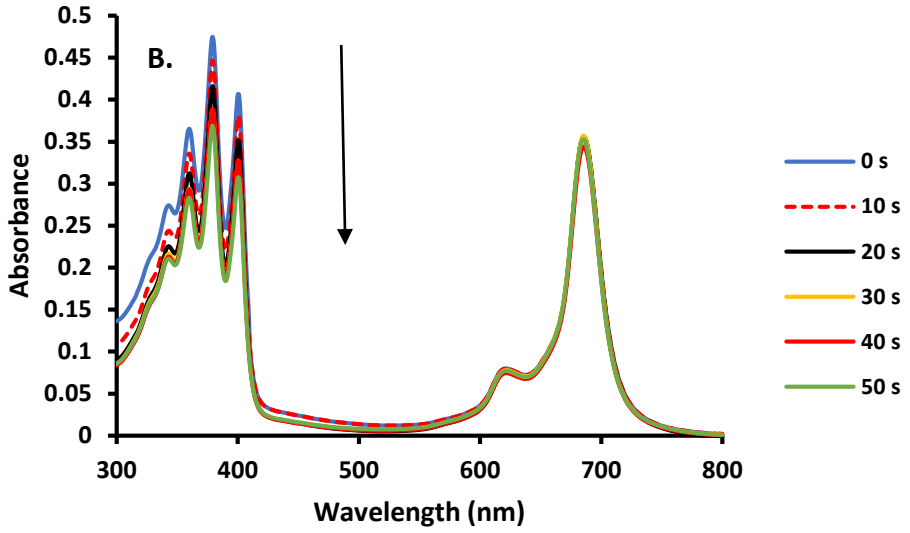

Figure 7: Absorption changes of (A) **2a** in DMSO and (B) **Q2a** in 0.2% DMSO.

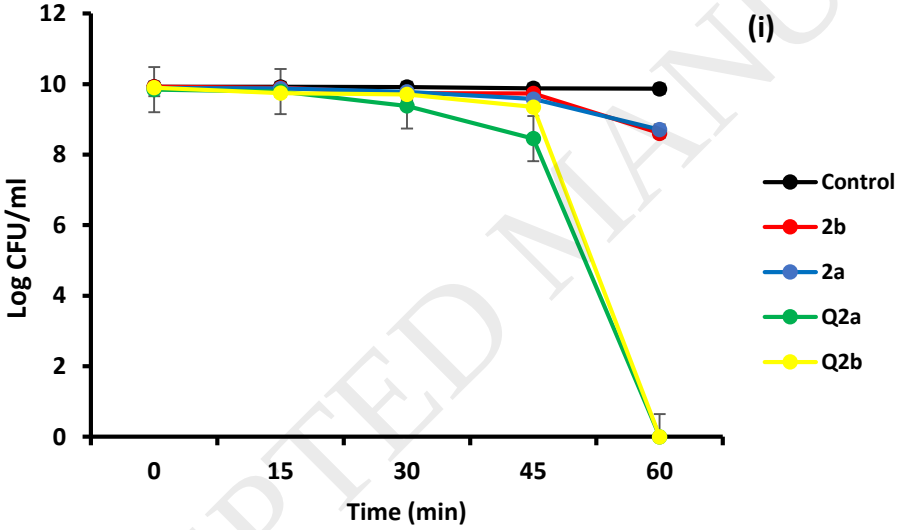

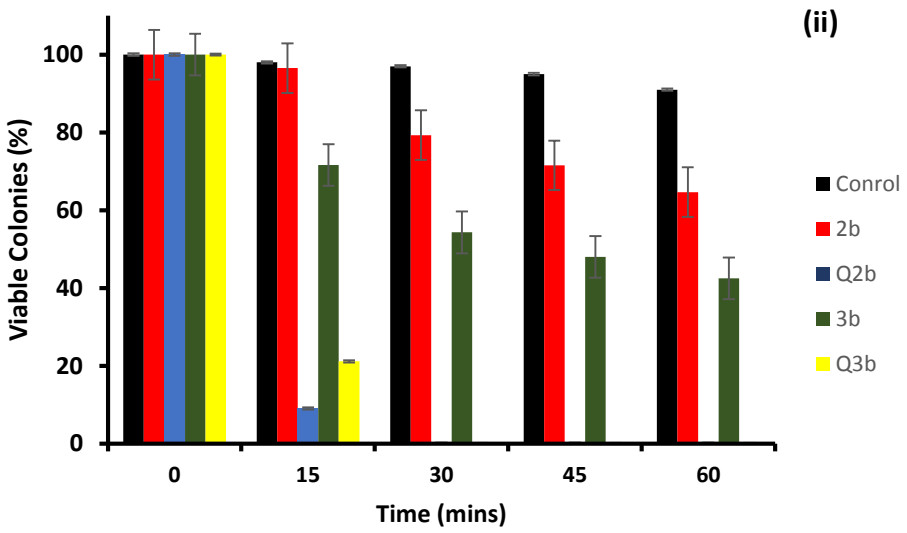

Figure 8: i) Survival curve of *E.coli* with 2.5 µM of **2a, 2b, Q2a** and **Q2b** and ii) Percentage reduction of *C. albican* of **2b, Q2b, 3b** and **Q3b**.

Table 1: The photophysical and photochemical properties summary in DMSO unless stated otherwise.

Compound	**Q-band** λ_{max} **(nm)**	Φ_F	τ_F **(ns)**	Φ_T	τ_T **(ns)**	Φ_Δ
1a	775[a] 745[a] 773	0.08	2.08	-	-	0.28
1b	739[a] 709[a] 738	0.09	5.48	-	-	0.20
2a	747	<0.01	1.86	-	-	0.54
2b	717	0.01	2.34	-	-	0.47
3a	765	<0.01	1.48	-	-	0.68
3b	736	<0.01	1.97	-	-	0.63
Q2a	684 687[b]	0.19 0.09[b]	1.92 0.71[b]	0.71 -	112 -	0.58 0.26[b]
Q2b	673 674[b]	0.24 0.11[b]	2.84 1.58[b]	0.66 -	292 -	0.50 0.23[b]
Q3a	702 704[b]	0.01 <0.01[b]	1.69 0.63[b]	0.92 -	76 -	0.66 0.38[b]
Q3b	685 687[b]	0.02 <0.01[b]	2.31 1.20[b]	0.87 -	92 -	0.62 0.32[b]

[a] values in DMF

[b] values in aqueous media (water containing 0.2% DMSO)

Table 2: Percentage reduction (log reduction) of all micro-organism in 0.2% DMSO (unless stated otherwise) after irradiating for 60 mins.

Sample	**Percentage reduction (log reduction)**		
	S. Aureus	***E. Coli***	***C. Albican***
2a	32.8 % (1.31)	16. 3 % (1.17)	60.2 % (1.59)
2b	48.6 % (1.45)	36.7 % (1.36)	68.5 % (1.78)
3a	27.1 % (1.28)	12.5 % (1.03)	35.6 % (1.36)
3b	30.4 % (1.30)	23.7 % (1.21)	40.3 % (1.40)
Q2a	100.0 % (8.42) 100.0 % (8.21)[a]	100.0 % (9.90) 100.0 % (9.43)[a]	100.0 % (7.94) 100.0 % (7.49)[a]
Q2b	100.0 % (8.37) 100.0 % (8.19)[a]	100.0 % (9.84) 100.0 % (9.38)[a]	100.0 % (7.87) 100.0 % (7.34)[a]
Q3a	100.0 % (8.57) 100.0 % (8.28)[a]	100.0 % (9.92) 100.0 % (9.41)[a]	100.0 % (7.98) 100.0 % (7.53)[a]
Q3b	100.0 % (8.48) 100.0 % (8.22)[a]	100.0 % (9.87) 100.0 % (9.36)[a]	100.0 % (7.92) 100.0 % (7.37)[a]

[a] the second values are in water (containing no DMSO)